On geothermometer and oxygen barometer using coexisting Fe-Ti oxides on a thermodynamic basis: A case of regular solution approximation*

Tetsumaru Itaya [1), 2)]

Abstract Using the experimental data of Buddington and Lindsley (1964), an attempt was made to develop Fe-Ti oxide geothermometer and oxygen barometer based on equilibrium thermodynamic methods. In this method, a regular solution approximation was adopted for the hematite-ilmenite solid solution (α phase) and the magnetite-ulvöspinel solid solution (β phase). Geothermometer and oxygen barometer have been shown in two ways. One method is to read from the graph, and the other is numerical formulation. Within the Buddington and Lindsley experimental conditions, the uncertainty of the geothermometer and oxygen barometer is ± 11°C for temperature and ± 0.32 at log f_{O_2}. The maximum difference between equilibrium temperature and oxygen fugacity estimated by the graphical method of Buddington and Lindsley and the thermodynamic methods using the chemical composition of naturally coexisting ilmenite and magnetite is so far 180°C for temperature and 5 at log f_{O_2}.

1. Introduction

Fe-Ti oxide minerals are common in metamorphic and igneous rocks. Their stability and paragenesis have been studied in detail experimentally. Buddington and Lindsley (1964) proposed a method to estimate the equilibrium temperature and oxygen fugacity using the mineral chemistry of hematite-ilmenite system (α phase) and magnetite-ulvöspinel system (β phase) when both phases coexist in equilibrium. The method is to read the equilibrium temperature and oxygen fugacity from the intersection of isoconcentration lines of both phases on the temperature vs. oxygen fugacity diagram obtained by the experiment (see Fig. 5 of Buddington and Lindsley, 1964). The method has the disadvantage that the reading error becomes large when the two curves are close to parallel. The experiments by Buddington and Lindsley have been performed with NNO ($Ni + 1/2O_2 = NiO$), FMQ ($3Fe_2SiO_4 + O_2 = 2Fe_3O_4 + 3SiO_2$) and WM ($6FeO + O_2 = 2Fe_3O_4$) oxygen fugacity buffers (Fig. 1). In the WM buffering experiment, the composition changes of both α and β phases are hardly seen within the range of experimental accuracy, so the drawing of isoconcentration lines for each phase is limited to the area in the NNO and FMQ buffering experiment. It is difficult to estimate the temperature and oxygen fugacity when moving away from the area. In recent years, attempts have been made to formulate geothermometer and oxygen barometer that use coexisting Fe-Ti oxide minerals based on thermodynamics. For example, Powell and Powell (1977) formulated them in the assumption as an ideal solution for the β phase and the scope of Henry's law for the amount of Fe_2O_3 in the α phase. Katsura *et al.* (1975) proposed the ideal solution approximation for the β phase in the temperatures of 1200-1300°C. However, in the experimental temperature range (500-1000°C) of Buddingtom and Lindsley, the ideal solution approximation to the β phase with an immiscible region might cause large errors. There are also many problems in applying Henry's law to the α phase.

In this paper, we assume a regular solution for both α and β phases, and formulate a geothermometer and an oxygen barometer using the experimental data of Buddington and Lindsley (1964) because the introduction of regular solutions allows us to treat the phases having immiscible regions.

---

* A publisher in England asked the author to translate a paper entitled "On a geothermometer and an oxygen barometer using coexisting Fe-Ti oxides on a thermodynamic basis: A case of regular solution approximation" that was written in Japanese. It is by the author who published it in *"The Journal of the Japanese Association of Mineralogists, Petrologists and Economic Geologists."* (vol. 75, pages 69-76, 1980). This is of its translation in English in which the figures and tables including the equations are reprinted from the original paper. This reprinting was permitted by Japan Association of Mineralogical Sciences. The author thanks Professor Hironobu Hyodo of Okayama University of Science and Dr. Takafumi Sonehara of Hiruzen Institute for Geology and Chronology who improved the manuscript to clear one.

E-mail: tetsumaru.itaya@gmail.com
1) Engineering Geology Center, Hiruzen Institute for Geology and Chronology, Co., Ltd.
2-12 Nakashima, Naka-ku, Okayama 703-8252, Japan

2) Japan Geochronology Network, NPO
2-12 Nakashima, Naka-ku, Okayama 703-8252, Japan

Received on March 8, 2021; Accepted on May 31, 2021.

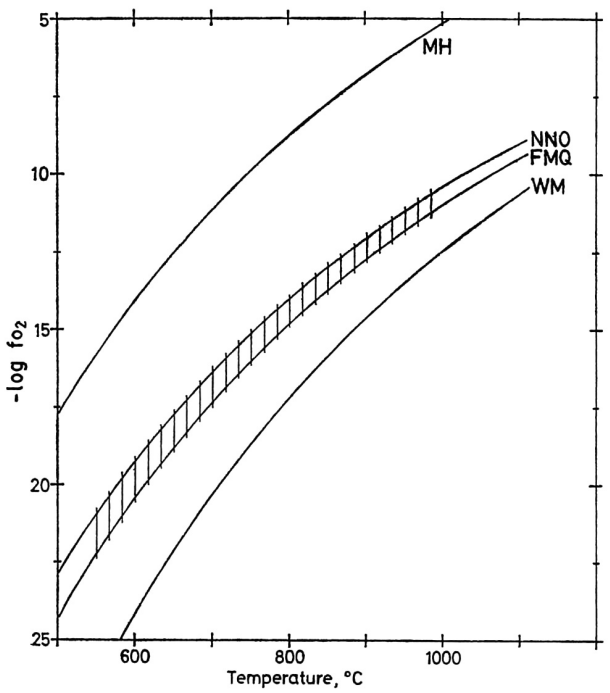

Fig. 1 Temperature vs. log fO_2 map for four oxygen buffer assemblages. Hatched area shows a temperature – oxygen fugacity region where the geothermometer and oxygen barometer of Fe-Ti oxides by Buddington and Lindsley (1964) are effective. The NNO, FMQ, WM and MH ($2Fe_3O_4 + 1/2O_2 = 3Fe_2O_3$) buffer lines are from Eugster and Wones (1962), corrected for total pressure of 2000 bar.

2. Geothermometer and Oxygen barometer

When the α and β phases coexist in equilibrium in the Fe-Ti-O system, some equations of the reaction relationship can be arbitrarily written. One is of the partition reaction, in which oxygen is not involved in the reaction (Eq. 1). If oxygen is involved in the reaction, they are of the β-phase oxidation reactions (Eqs. 2, 3 and 4).

$$FeTiO_3 + Fe_3O_4 = Fe_2O_3 + Fe_2TiO_4 \quad (1)$$

$$4\,Fe_3O_4 + O_2 = 6\,Fe_2O_3 \quad (2)$$

$$4\,Fe_2TiO_4 + O_2 = 4\,FeTiO_3 + 2\,Fe_2O_3 \quad (3)$$

$$6\,Fe_2TiO_4 + O_2 = 2\,Fe_3O_4 + 6\,FeTiO_3 \quad (4)$$

The following equations show an equilibrium relation of the equation 1.

$$\ln\left(\frac{a_{hm}}{a_{il}}\right)^{\alpha} \Big/ \left(\frac{a_{mt}}{a_{ul}}\right)^{\beta} = \frac{-\Delta G_1}{RT} = \frac{-\Delta H_1}{RT} + \frac{\Delta S_1}{R} \quad (5)*$$

*hm: hematite, il: ilmenite, mt: magnetite, ul: ulvöspinel

$$\ln\left(\frac{X_{hm}}{X_{il}}\right)^{\alpha} \Big/ \left(\frac{X_{mt}}{X_{ul}}\right)^{\beta} + \ln\left(\frac{\gamma_{hm}}{\gamma_{il}}\right)^{\alpha} \Big/ \left(\frac{\gamma_{mt}}{\gamma_{ul}}\right)^{\beta} = \frac{-\Delta H_1}{RT} + \frac{\Delta S_1}{R} \quad (6)$$

Here, ΔG_1, ΔH_1 and ΔS_1 are the reaction free energy, enthalpy and entropy changes, respectively. a_i, X_i and γ_i are the activity, mole fraction and activity coefficient of the i component of each phase, respectively. R is the gas constant and T is the temperature. If assuming a regular solution for both α and β phases, the relationship between the activity coefficient γ_i and the mole fraction X_i gives the following equation (Prigogine and Defay, 1950).

$$\ln \gamma_i = (1 - X_i)^2 \frac{W}{RT} \quad (7)$$

Here, W is a parameter that characterizes the regular solution. In general, W is a function of temperature, but in this paper, we assume that it is constant. Substituting the equation 7 into the equation 6 and rearranging them gives the following equations.

$$(1-2X_{hm})W^{\alpha} - (1-2X_{mt})W^{\beta} + \Delta H_1 - T\Delta S_1 = -RT\ln\frac{X_{hm}(1-X_{mt})}{X_{mt}(1-X_{hm})} \quad (8)$$

$$T = \{(1-2X_{hm})W^{\alpha} - (1-2X_{mt})W^{\beta} + \Delta H_1\}/(\Delta S_1 - R\ln\frac{X_{hm}(1-X_{mt})}{X_{mt}(1-X_{hm})}) \quad (9)$$

Here, the superscripts α and β of W indicate α and β phases, respectively.

In addition, the following equation shows an equilibrium relation of the equation 2.

$$\ln\frac{a^6_{hm}}{a^4_{mt}\cdot fo_2} = \frac{-\Delta G_2}{RT} = \frac{-\Delta H_2}{RT} + \frac{\Delta S_2}{R} \quad (10)$$

$$\ln\frac{X^6_{hm}}{X^4_{mt}\cdot fo_2} + \ln\frac{\gamma^6_{hm}}{\gamma^4_{mt}} = \frac{-\Delta H_2}{RT} + \frac{\Delta S_2}{R} \quad (11)$$

Substituting the equation 7 into the equation 11 and rearranging them gives the following equations.

$$6(1-X_{hm})^2 W^{\alpha} - 4(1-X_{mt})^2 W^{\beta} + \Delta H_2 - T\Delta S_2 = -RT\ln\frac{X^6_{hm}}{X^4_{mt}\cdot fo_2} \quad (12)$$

$$\ln fo_2 = \{6(1-X_{hm})^2 W^{\alpha} - 4(1-X_{mt})^2 W^{\beta} + \Delta H_2 - T\Delta S_2\}/RT + \ln\frac{X^6_{hm}}{X^4_{mt}} \quad (13)$$

If the six thermodynamic parameters of W^{α}, W^{β}, ΔH_1, ΔS_1, ΔH_2 and ΔS_2 are known, the temperature (see Eq. 9) and oxygen fugacity (see Eq. 13) are functions of the composition of the coexisted α and β phases. However, at present, other parameters except for ΔH_2 and ΔS_2 are unknown.

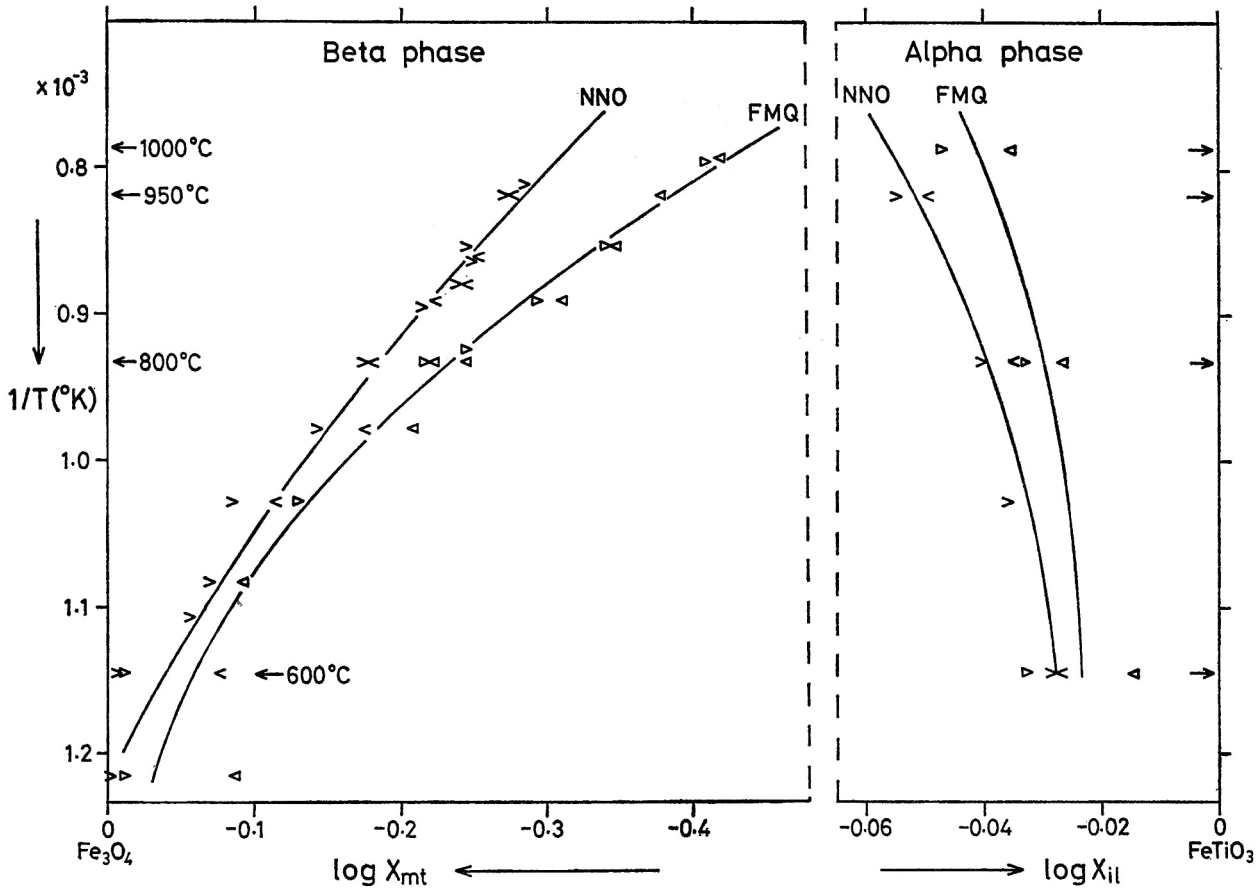

Fig. 2 The $1/T$ – log X map created from Figs 2 and 3 of Buddington and Lindsley (1964). The solid lines are the least squares approximation curves by the second-order polynomial.

3. Calculation of thermodynamic parameters

In the equations 8 and 12, there are the experiments by Buddington and Lindsley (1964) among X_{hm}, X_{mt} and T, and the experiments by Eugster and Wones (1962) for f_{O_2}. So, both equations show a four simultaneous equation with four unknowns, W^{α}, W^{β}, ΔH_i and ΔS_i. If there are n different experimental results, we get n four-element linear equations. If n=4 or more, four unknown solutions can be obtained independently in both equations.

Buddington and Lindsley's experimental results (read from their Figs. 2 and 3) were re-plotted on the $1/T$ - log Xi diagram for the purpose of selecting the values needed to proceed with the above calculations (Fig. 2).

The solid lines in the figure are the least squares approximation curves by the second-order polynomial. The experimental results by the WM buffer method were not used because of the large error. Experiments on the α phase of Buddington and Lindsley have been performed with both NNO and FMQ buffering methods at only three different temperatures (NNO: 600, 800, 950°C, FMQ: 600, 800, 1000°C). Therefore, we decided to obtain the experimental results of the β phase, which corresponds to the experimental temperature of the α phase, from the least squares approximation curve. The six sets of data selected are shown in Table 1.

When substituting the six sets of numerical values in Table 1 into the equations 8 and 12 and obtaining the solutions of W^{α}, W^{β}, ΔH_i and ΔS_i independently by the least squares approximation method of four-element simultaneous linear equations, as a result, appropriate values could not be obtained for each parameter because

Table 1 Six sets of data of coexisting α and β phases selected to calculate thermodynamic parameters (see text). The values of log f_{O_2} in the experimental temperatures are also shown in this table.

T(°C)	X_{mt}	X_{hm}	log fo_2	Oxygen buffer s.
950	0.5200	0.1117	-11.19	NNO
800	0.6534	0.0860	-14.00	
600	0.9122	0.0620	-19.26	
1000	0.3656	0.0898	-10.98	FMQ
800	0.5846	0.0661	-14.83	
600	0.8725	0.0498	-20.45	

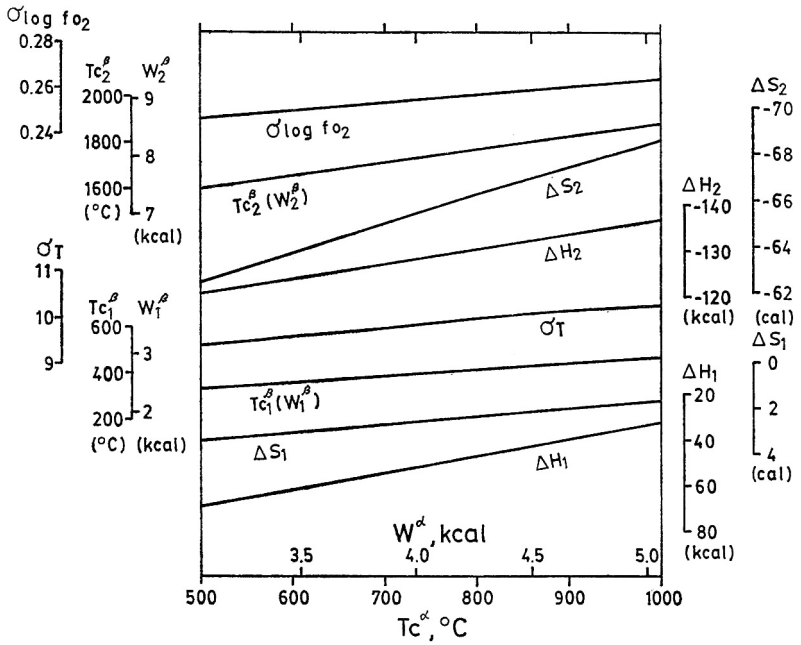

Fig. 3 Thermodynamic parameters calculated by the least square approximation method of the equations 1 and 2 (see text). This figure also shows the standard deviation of temperature and log f_{O_2} as described later. The figure shows the variation of the value of each calculated parameter around the critical temperature of α phase ($T_c{}^{\alpha}$ = 750°C).

there were many unknowns compared to the number of sets of numerical values to be substituted. Therefore, as a method of reducing the number of unknown parameters, we estimated the W value from the phase diagram. In the case of regular solutions, there is the following relationship between the critical temperature (T_c) and W in the immiscible region (Prigogine and Defay, 1950).

$$W = 2RT_c \tag{14}$$

Fortunately, it is known from the experiment of Lindsley (1973) that the critical temperature ($T_c{}^{\alpha}$) of the α phase is 750 ± 50°C. The temperature ($T_c{}^{\beta}$) of the β phase is about 450°C that has been predicted by Vincent *et al.* (1957). Fig. 3 shows the thermodynamic parameters (W^{β}, ΔH_i and ΔS_i) calculated by the least square approximation method of three-dimensional simultaneous linear equations for the equations 1 and 2 at fixed W^{α} ($T_c{}^{\alpha}$ = 750°C). The figure also shows the variation of the value of each calculated parameter around the critical temperature ($T_c{}^{\alpha}$ =750°C). When W^{α} is estimated as 4066 cal/mol ($T_c{}^{\alpha}$ = 750°C) and W^{β} as 2874 cal/mol ($T_c{}^{\beta}$ = 450°C), ΔH_1 and ΔS_1 are calculated by the least squares approximation method of the two-dimensional simultaneous linear equations. Fig. 4 shows the variation of the value of each calculated parameter around the critical temperature ($T_c{}^{\beta}$ = 450°C).

Substituting the obtained thermodynamic parameters and X_{hm} and X_{mt} in Table 1 into the equations 9 and 13, the temperature and oxygen fugacity are calculated. The calculated temperature and fugacity can be compared with the experiments. The dispersions (σT and $\sigma \log f_{O_2}$) of temperature and oxygen fugacity are calculated by the following equations. In Figs. 3 and 4, these dispersions are also shown.

$$\sigma_T = \frac{\sum_{i=1}^{n} (T_i{}^{e} - T_i{}^{c})^2}{n-1} \tag{15}$$

$$\sigma_{\log fo_2} = \frac{\sum_{i=1}^{n} \{(\log fo_2)_i{}^{e} - (\log fo_2)_i{}^{c}\}^2}{n-1} \tag{16}$$

Here, T^e and $(\log f_{O_2})^e$ are the experimental values, and T^c and $(\log f_{O_2})^c$ are the calculated values.

These calculated thermodynamic parameters (ΔH_i, ΔS_i, σT and $\sigma \log f_{O_2}$) have small change within the variation (± 100°C) of the critical temperature of both α and β phases (Figs 3 and 4). Table 2 shows the values of W^{α}, W^{β}, ΔH_i, ΔS_i, σ_T and $\sigma_{\log f_{O_2}}$ at $T_c{}^{\alpha}$ = 750°C and $T_c{}^{\beta}$ = 450°C. This table also shows the calculated parameters of ΔH_i, ΔS_i and $\sigma_{\log f_{O_2}}$ for the oxidation reactions (Eqs. 3 and 4). The standard enthalpy and entropy changes of each reaction calculated from the

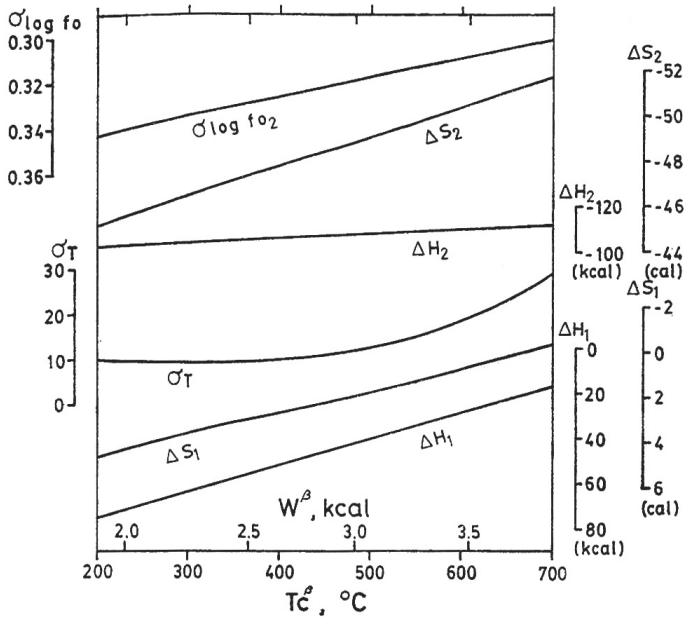

Fig. 4 Thermodynamic parameters calculated by the least square approximation method of the equations 1 and 2 (see text). This figure also shows the standard deviation of temperature and log f_{O_2} as described later. The figure shows the variation of the value of each calculated parameter around the critical temperature of β phase ($T_c{}^{\beta}$ = 450°C).

Table 2 Thermodynamic parameters (ΔH_i and ΔS_i) calculated by the least square approximation method (see text) after recognizing W^{α} (4066 cal/mol) and W^{β} (2874 cal/mol). The values of σT and $\sigma \log f_{O_2}$ are also shown (see text for the calculation method). The values in parenthesis are from thermochemical data of Robie and Waldbaum (1968) and Ono and Moriyama (1973).

	Eq.1	Eq.2	Eq.3	Eq.4
W^{α}(cal/mol)	4066	4066	4066	4066
W^{β}(cal/mol)	2874	2874	2874	2874
ΔH(kcal)	4623 (4295)	-113.6 (-114.2)	-132.0 (-131.4)	-141.3 (-140.0)
ΔS(cal)	2.172 (-0.343)	-48.44 (-67.78)	-57.13 (-66.40)	-61.47 (-65.72)
σ_T	11			
$\sigma \log fo_2$		0.32	0.32	0.33

thermal data of Robie and Waldbaum (1968) and Ono and Moriyama (1973) are also shown in parenthesis of Table 2 for comparison, indicating that ΔH_i and ΔS_i of the oxidation reactions (Eqs. 2, 3, 4) and ΔH_i of the partition reaction are in good agreement with the values calculated from the thermal data.

As a way to proceed with the calculation by reducing the number of unknown parameters, ΔH_i and ΔS_i may be estimated instead of estimating W^{α} and W^{β}. However, ΔH_i and ΔS_i are accurately known in the oxidation reaction (Eq. 2) and not well in the partition reaction (Eq. 1). There is a large difference between the cases where W^{α} and W^{β} obtained by estimating ΔH_i and ΔS_i are for the equations 1 and 2, respectively.

Furthermore, when the partition reaction (Eq. 1) and the oxidation reaction (Eq. 2) are combined into one reaction formula, W^{α} and W^{β} obtained by estimating ΔH_i and ΔS_i take abnormal values and extremely large σT and $\sigma \log f_{O_2}$ values. At present, the methods using other than estimated W^{α} and W^{β} are not suitable.

4. Discussion

When substituting the thermodynamic parameters (W^{α}, W^{β}, ΔH_i and ΔS_i of Eqs. 1 and 2 in Table 2) into the equations 9 and 13, the temperature (T) and the oxygen fugacity (log f_{O_2}) are given in the following equations.

$$T = \frac{2893X_{mt} - 4092X_{hm} + 2926}{1.0932 - \ln \dfrac{X_{hm}(1 - X_{mt})}{X_{mt}(1 - X_{hm})}} \ (°\mathrm{K}) \qquad (17)$$

$$\ln fo_2{}^* = \{4.244(X_{hm}{}^2 - 2X_{hm}) - 2(X^2{}_{mt} - X_{mt}) - 17.511\}X + \ln \frac{X^6{}_{hm}}{X^4{}_{mt}} + 24.374 \qquad (18)$$

$$X = \frac{1.0932 - \ln \dfrac{X_{hm}(1 - X_{mt})}{X_{mt}(1 - X_{hm})}}{X_{mt} - 1.4148X_{hm} + 1.0117}$$

The estimation error of temperature and oxygen fugacity obtained using the composition of coexisting α and β phases would be equivalent to the dispersion values calculated from the equations 15 and 16. Within the experimental temperature range conducted by

*The equations for log f_{O_2} can be obtained from the equations 3 and 4 too. The values calculated using the three different oxidation reactions are completely the same.

*For Eq. 3

$$\ln fo_2 = \{4.2443(X^2{}_{hm} - 0.6667X_{hm}) - 2X^2{}_{mt} - 21.557\}X + \ln \frac{(1-X_{hm})^4 \cdot X^2{}_{hm}}{(1-X_{mt})^4} + 28.747$$

*For Eq. 4

$$\ln fo_2 = \{4.2443X^2{}_{hm} - 2(X^2{}_{hm} - X_{mt}) - 23.581\}X + \ln \frac{X^2{}_{mt}(1 - X_{hm})^6}{(1 - X_{mt})^6} + 30.933$$

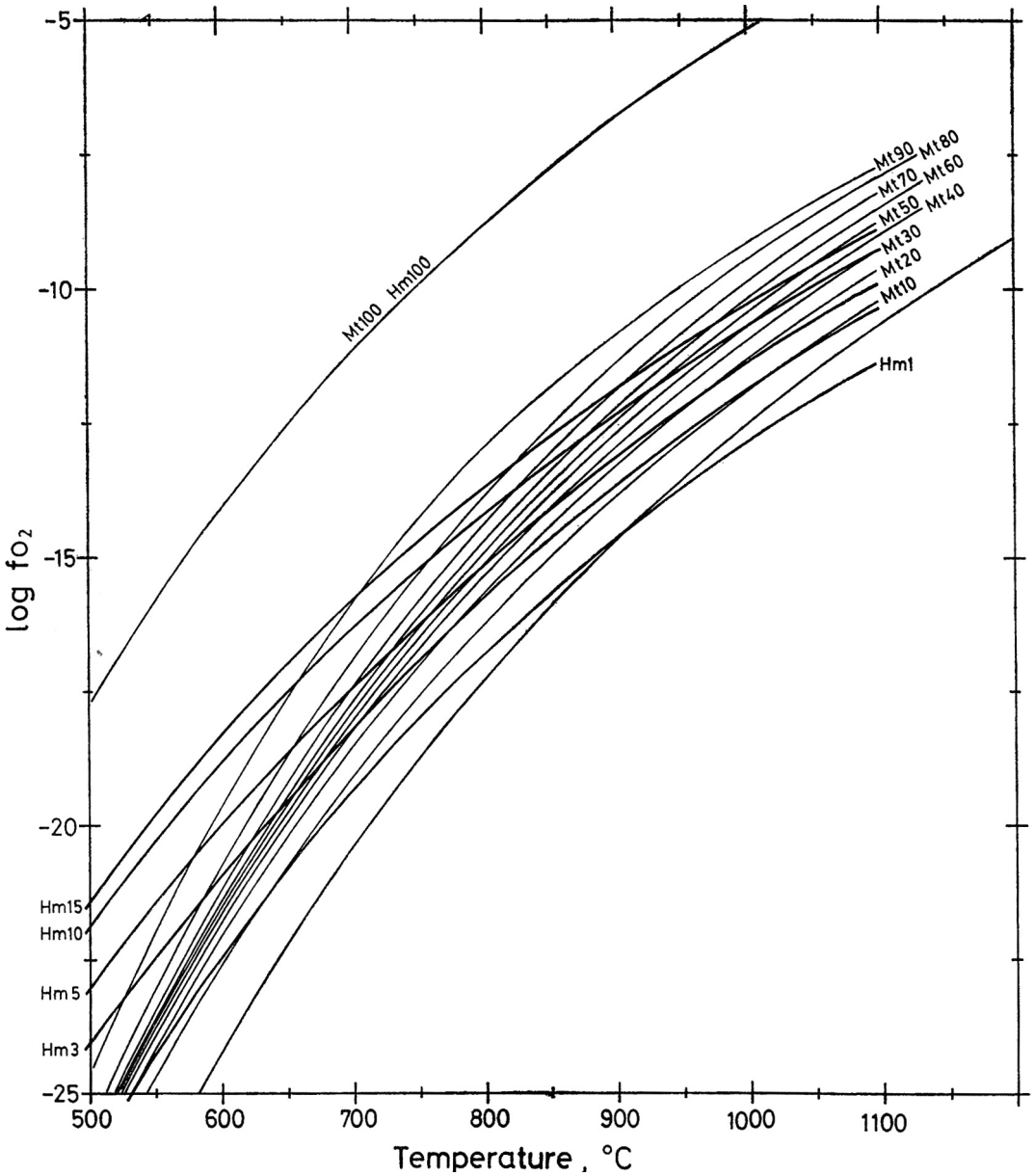

Fig. 5 Temperature vs. log f_{O_2} – X diagram created using the Equations 17 and 18. This figure is very similar to the figure (Fig. 5) of Buddington and Lindsley (1964).

Buddington and Lindsley (1964), the errors of the temperature and the log f_{O_2} are ± 11°C and ± 0.32, respectively as seen in Table 2. Fig. 5 shows T – log f_{O_2}–X map created using the equations 17 and 18. This figure is very similar to the figure (Fig. 5) of Buddington and Lindsley (1964) and shows the characteristics caused by the existence of immiscible regions. For example, the β-phase isoconcentration lines tend to be dense in the temperatures close to 450°C, and the α-phase isoconcentration lines tend to become denser as Fe_2O_3 mol increases.

In the past, Fig. 5 of Buddington and Lindsley (1964) has been cited by many researchers who have estimated the equilibrium temperature and oxygen fugacity of the igneous rocks and metamorphic rocks using the composition of the coexisting magnetite and ilmenite. Fig. 6 compares the temperature and oxygen fugacity (open circles) estimated by the researchers and the values (solid circles) calculated by the present paper. The two circles are connected by a solid line. Analytical data for naturally coexisting magnetite and ilmenite were from Buddington and Lindsley (1964), Carmichael (1966), Mathison (1975) and Himmelberg and Ford (1977). The solid lines are short in the area between the NNO and FMQ lines around 800°C, indicating that the two methods are in good agreement with each other. On the other hand, the solid lines are long in the areas far from the NNO line and the FMQ line, indicating that the two methods are in poor agreement. The maximum differences are 180°C for temperature and 5 for log f_{O_2}. As a general property of the

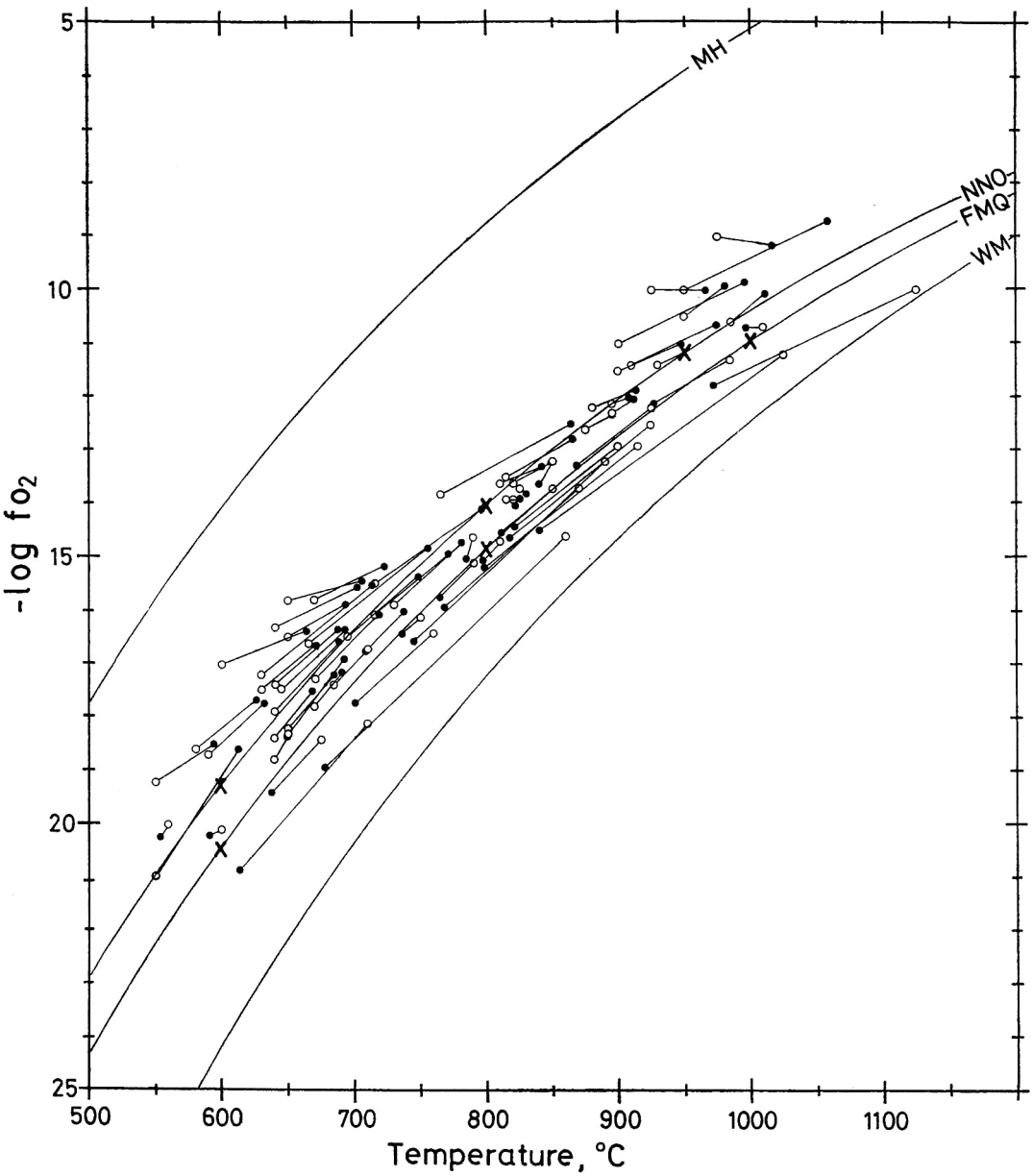

Fig. 6 Diagram showing the difference of the equilibrium temperature and oxygen fugacity estimated by the graphical method of Buddington and Lindsley (1964) and the present thermodyanamic method. Open circle shows the temperature and log f_{O_2} position by the former method and solid circle, by the latter method. Composition data of natural coexisting ilmenite and magnetite are of Buddington and Lindsley (1964), Carmichael (1966), Mathison (1975) and Himmelberg and Ford (1977). "X" shows the six data points of temperature and log f_{O_2} (see Table 1) that was used in the calculation of thermodynamic parameters.

difference by the two methods, in the log f_{O_2} region lower than the FMQ line, the open circles shift to higher log f_{O_2} and temperature sides. On the contrary, in the higher log f_{O_2} region than the NNO line, the open circles shift to lower log f_{O_2} and temperature sides. At present, it has not yet been possible to quantitatively discuss the differences in temperature and oxygen fugacity estimated by both methods. In this respect, there are still unsolved parts regarding this problem. However, by using both estimation methods critically along with petrological studies of natural rock samples, the advantages and disadvantages of both will become clear.

5. Summary

An attempt was made to formulate a Fe-Ti oxide mineral geothermometer and an oxygen barometer based on thermodynamics using the experimental data of Buddington and Lindsley (1964). In this attempt, regular solutions were assumed for the hematite-ilmenite solid solution (α phase) and magnetite-ulvöspinel solid solution (β phase). Within the experimental temperature range conducted by Buddington and Lindsley (1964), the errors are $\pm$ 11°C for temperature and $\pm$ 0.32 for log f_{O_2}. The equilibrium temperature and oxygen fugacity estimated from the chemical composition of naturally

coexisting ilmenite and magnetite often makes a big difference between the graphical method of Buddington and Lindsley (1964) and the thermodynamic method described in this paper. Its maximum value is 180°C for temperature and 5 for log fO_2.

Acknowledgments

This research was started by being proposed from Associate Professor Shohei Banno while the author was a graduate student at Graduate School, Kanazawa University (1974-1976). The author would like to thank Professor Yoshio Ueda and Associate Professor Hitoshi Onuki (currently Professor of Earth Sciences, Faculty of Science, Hirosaki University) for their continued encouragement in advancing the research. The author thanks Associate Professor Shohei Banno of Kanazawa University for his appropriate guidance and advice in the content discussion in writing this paper. FACOM (230-38) of Tohoku University Computer Center was used for a series of calculation processes related to this research.

References

Buddington, A.F. and Lindsley, D.H. (1964) Iron titanium oxide minerals and synthetic equivalents. *Journal of Petrology*, **5**, 310-357.

Carmichael, I.S.E. (1966) The iron-titanium oxides of salic volcanic rocks and their associated ferromagnesian silicates. *Contributions to Mineralogy and Petrology*, **14**, 36-64.

Eugster, H.P. and Wones, D.R. (1962) Stability relations of the ferruginous biotite and annite. *Journal of Petrology*, **3**, 82-125.

Himmelberg, G.R. and Ford, A.B. (1977) Iron-titanium oxides of the Dufek intrusion, Antarctica. *American Mineralogist*, **62**, 623-633.

Katsura, T., Wakihara, M. Hara, S. and Sugihara, T. (1975) Some thermodynamic properties in spinel solid solutions with the Fe3O4 component. *Journal of Solid State Chemistry*, **13**, 107-113.

Lindsley, D.H. (1973) Delimitation of the hematite-ilmenite miscibility gap. *Geological Society of America Bulletin*, **84**, 657-662.

Mathison, C.I. (1975) Magnetites and ilmenites in the Somerset Dam layered basic intrusion, southeastern Queensland. *Lithos*, **8**, 93-111.

Ono, K. and Moriyama, J. (1973) Thermodynamic Study on the Fe-FeO-TiO_2 System. *Journal of the Mining and Metallurgical Institute of Japan*, **89**, 313-316 (in Japanese with English abstract).

Powell, R. and Powell, M. (1977) Geothermometry and oxygen barometry using coexisting iron-titanium oxides: a reappraisal. *Mineralogical Magazine*, **41**, 257-263.

Prigogine, I. and Defay, R. (1950) *Thermodynamique Chimique*, Ediotions Desoer, Liege, Translated by Senoo (1966) *Chemical Thermodynamics* (2 volumes) Misuzu Shobo, Ltd., Tokyo, 549pp (in Japanese)

Robie, R.A. and Waldbaum, D.R. (1968) Thermodynamic properties of minerals and related substances at 298.15°K (25.0°C) and one atmosphere (1.013 bars) pressure and at higher temperatures. *United States Geological Survey Bulletin*, **1259**, 256p.

Vincent, E.A., Wright, J.B., Chevallier, R. and Mathieu, S. (1957) Heating experiments on some natural titaniferous magnetites. *Mineralogical Magazine*, **31**, 624-655.

地質技術 第 11 号，19-26 頁（2021）

Fe-Ti 酸化鉱物の地質温度計と酸素分圧計の数式化について―正則溶液モデルの場合―

板谷徹丸 [1), 2)]

[1)] 株式会社蒜山地質年代学研究所（地質技術センター）
〒 703-8252 岡山市中区中島 2 番地 12

[2)] NPO 法人地球年代学ネットワーク
〒 703-8252 岡山市中区中島 2 番地 12

日本語要旨　Buddington and Lindsley（1964）の実験データを使用して，平衡熱力学的方法に基づいたFe-Ti酸化物地質温度計と酸素分圧計の開発が試みられた．この方法では，ヘマタイト-イルメナイト固溶体（α相）とマグネタイト-ウルボスピネル固溶体（β相）に正則溶液近似が行われた．地質温度計と酸素分圧計は二つの方法で示した．一つはグラフから読み取る方法である．他は数値的に定式化した．Buddington and Lindsleyの実験条件範囲内では，地質温度計と酸素分圧計の不確かさは，温度で±11℃，log fO_2で±0.32である．天然に共存するイルメナイトとマグネタイトの化学組成を使用してBuddington and Lindsleyのグラフ法と熱力学的方法によって推定された平衡温度と酸素フガシティーの最大差は，これまでのところ温度で180℃，log fO_2で5である．